**SUPERCAPACITY OF TITANIUM CARBIDE DERIVED CARBON OBTAINED BY FLUORINATION**

*Nicolas Batisse, Katia Guérin, Marc Dubois, André Hamwi*

Laboratoire des Matériaux Inorganiques UMR UBP-CNRS 6002, Clermont Université, Clermont-Ferrand, FRANCE

## Introduction

Since a decade, a new way to produce nanoporous carbons consists in chlorination of carbide in order to etch metallic atoms and to leave the carbon matrix [1]. Gaseous molecular chlorine reacts with metallic atoms at high temperature (600 – 900°C) to form most of the time a gaseous chloride which is easily removed and carbon called carbide derived carbon (CDC). The unique nanoporous structure of CDC together with the narrow pore size distribution and possibility to tune the pore size distribution [2,3] has noticeably forced the development of applications requiring the nanoporous materials such as fuel cells, adsorption processes, hydrogen storage…. One of the most challenging applications is the rapidly developing field of the electrochemical energy storage devices such as super- or ultracapacitors [4]. Up to now, the best CDC materials for supercapacitors have been made from chlorination of titanium carbide [5]. However, such materials present some disavantages: the highest being their synthesis temperature which is about 800°C. Another way of halogenation can be studied in order to decrease the synthesis temperature and to obtain another pore size distribution: fluorination [6]. In order to set the fluorination conditions of titanium carbide such as the temperature and the optimal carbide/fluorine ratio, some thermodynamical calculations have been conducted and exhibit the potentiality of carbon formation at low temperatures with a high stoichiometric control required between fluorine gas and solid carbide, in comparison with chlorination. The first carbon material prepared by fluorination under pure fluorine gas was characterized by XRD, $N_2$ sorption at 77K, and solid state $^{13}$C NMR. Its electrochemical behaviour as electrode material in supercapacitor was investigated by cyclic voltammetry.

## Experimental Methods

Titanium carbide powder with particle size of 2 µm was obtained from Alfa Aesar. For fluorination under 1 atm of pure fluorine gas stream (process called direct fluorination), the fluorine flow was set between 10 and 21 mL.min$^{-1}$ and the fluorination temperature at 130°C. Prior to and after fluorination the material was outgassed at 130°C under nitrogen gas for 2 hours. Then, the synthesis tube was set in a glove box to prevent reaction with air of the formed CDC.

The chemical analysis of the crystallised phases has been made by quantitative X-ray diffraction XRD. Powder XRD measurements were performed using a PHILIPS XPERT diffractometer with a Cu($K_\alpha$) radiation. A special seal diffraction cell was used which allows the conditioning of the material in a glove box. NMR experiments were carried out with Bruker Avance spectrometer, with working frequencies for $^{13}$C of 73.4 MHz, respectively. A Magic Angle Spinning (MAS) probe (Bruker) operating with a 4 mm rotor was used. For MAS spectra, a simple sequence was performed with a single π/2 pulse length of 3.5 µs for $^{13}$C. $^{13}$C chemical shifts were externally referenced to tetramethylsilane (TMS). Nitrogen adsorption isotherms were measured at 77 K by a MICROMERITICS ASAP 2020 automatic apparatus. Before measurements, samples were pre-treated under secondary vacuum at 300 C for 12h for sufficient removal of impurities. For electrochemical measurements, a mixture of 80wt% TiC-CDC, 10wt% carbon black and 10wt% polyvinylidene difluoride was stirred thoroughly in ethanol and then deposited at 50°C on stainless steel current collector disk. The capacitor was assembled in a two electrodes Swagelok type cell, including glassy paper as separator and 1M KOH as electrolyte solution. Voltammetry was performed at room temperature with a VMP2-Z instrument (Biologic).

## Results and Discussion

X-ray diffractogram (Figure 1) shows that, after fluorination, crystallized titanium carbide is still present at quantities higher than 5%. Cubic TiC with space group Fm-3m exhibits (111), (200), (220), (311) and (222) reflections at 2 theta equal to 35°9, 41°7, 60°4, 72°4, 76°1, respectively. Moreover, some peaks of titanium trifluoride are visible at 2 theta equal to 23°1, 47°0 as well as the superimposition of peaks predicted at 53°6 and 53°3. 4 peaks at 32°6, 38°7, 58°6 and 68°1 are not attributed but do not correspond to a titanium fluoride or oxyfluoride, a carbon fluoride or a crystallized carbon. XRD pattern does not reveal the presence of carbon or of almost crystallized carbon. Such information can be extracted from solid state $^{13}$C NMR.

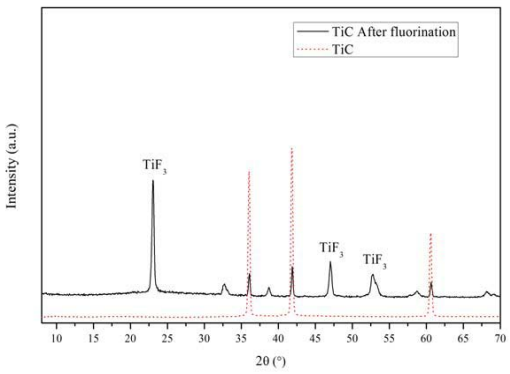


**Fig. 1** XRD pattern of titanium carbide before and after fluorination

Figure 2 shows MAS $^{13}$C-NMR spectrum of TiC-CDC obtained by fluorination. It exhibits a line at 121 ppm which can be assigned to $sp^2$ carbons as in graphite (for carbon in graphite $\delta$ = 118 ppm) [7]. In the case of fluorinated carbon, a line at 82-90 ppm, which is related to covalent C-F bonds, always appears. Because of the absence of this line, $^{13}$C NMR data prove the carbon formation and revokes the significant formation of fluorinated carbons. Solid state $^{19}$F-NMR confirmed that carbon fluoride is not formed because no broad line centered near -190 ppm, typical of C-F bonds in graphite fluoride, appears [7]. However, the spectra reveal the presence of an inorganic phase such as a titanium fluoride. Its spectrum is very broad (several hundred ppm) and consists in a set of superimposed isotropic lines and spinning sidebands.

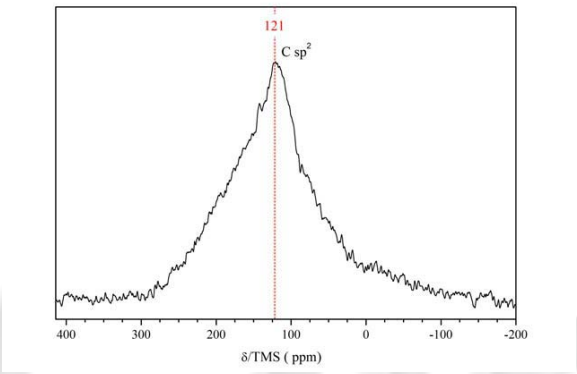


**Fig. 2** MAS $^{13}$C-NMR spectrum of titanium carbide after fluorination. The spinning rate is 10 kHz.

Quantitative XRD by Rietveld refinement with an inner silicium standard demonstrates that the material contains after fluorination 60, 11 and 28 % molar ratio of carbon, $TiF_3$ and TiC, respectively.

The $N_2$ sorption isotherms recorded at 77 K exhibits a little hysteresis loops, suggesting a low mesopore volumes which can be attributed to $TiF_3$ and TiC contents. Interestingly, a huge amount of $N_2$ is adsorbed at low relative pressure indicating microporous behaviour. Pore size distribution obtained by a DFT method of TiC–CDC prepared by fluorination shows that the carbon contains narrowly distributed micropore sizes centered at 0.57 nm. The BET SSA is 320 $m^2/g$ and the DFT micropore volume is of 0.17 $cm^3/g$.

To establish the suitability of TiC-CDC prepared by fluorination as supercapacitors, a study of EDLC characteristics was performed by using an aqueous-based electrolyte KOH. The cyclic voltammograms were recorded in the voltage range from -0.6 V to 0.6 V by using a potential scan rate of 10 $mV.s^{-1}$. The results are presented in figure 3. Even if the BET SSA is weak, the sub-microporosity allows to obtain non negligible supercapacity.

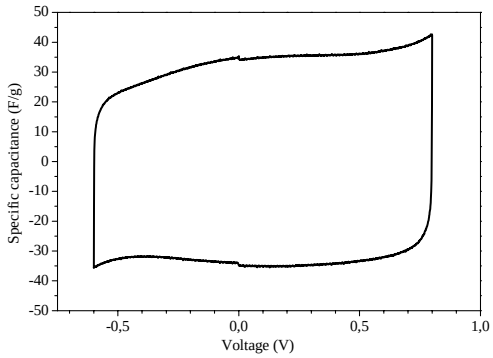


**Fig. 3** Cyclic voltammogram at a scan rate of 10$mV.s^{-1}$ of TiC-CDC in 1M KOH electrolyte

It was observed that the capacitor has a nearly rectangular shape of C-U curve, revealing a capacitive and conductive behaviour of the formed CDC. The gravimetric specific capacitance of about 70$F.g^{-1}$ is promising regarding the amount of carbon in the material and could be attributed to the well suited size of nanopores with the electrolyte ions one [8].

## Conclusions

For the first time TiC-CDC have been obtained by fluorination. This process occurs at low temperature contrary to the chlorination way. No carbon fluorides are formed but at this stage of the study, carbon is not purified and still contains TiC and titanium fluorides which induce some mesoporosity and $TiF_3$ could partially block the narrow-distributed sub-microporosity. A well-defined supercapacitor behaviour has been obtained. Further work on the purification of such CDC are under progress in order to increase the BET SSA and as a consequence to increase the supercapacity performances.

**References**

[1] Y. Gogotsi (Ed.), Nanomaterials Handbook, Taylor and Francis, 2006

[2] Leis J, Perkson A, Arulepp M, Käärik M, Svensson G. Carbon nanostructures produced by chlorinating aluminium carbide. Carbon. 2001;39(13):2043-8.

[3] Gogotsi Y, Nikitin A, Ye H, Zhou W, Fischer JE, Yi B, Floley HC, Barsoum MW. Nanoporous carbide-derived carbon with tunable pore size. Nat. Mater. 2003;2(9):591-4.

[4] Burke A. Ultracapacitors: why, how, and where is the technology. J. Power Sources. 2000;91(1):37-50.

[5] Arulepp M, Leis J, Lätt M, Miller F, Rumma K, Lust E, Burke AF. The advanced carbide-derived carbon based supercapacitor. J. Power Sources. 2006;162(2):1460-6.

[6] Fracassi F, d'Agostino R. Chemistry of titanium dry etching in fluorinated and chlorinated gases. Pure and Applied Chemistry. 1992; 64:703-707

[7] Panich AM, Vieth HM, Ummat PK, Datars WR. Solid state 19F NMR study of acceptor-doped fullerenes (MF6)2C60 (M=As, Sb). Physica B: Condensed Matter. 2003;327(1):102-7.

[8] Chmiola J, Yushin G, Dash R, Gogotsi Y. Effect of pore size and surface area of carbide derived carbons on specific capacitance. J. Power Sources. 2006;158(1):765-72.